Supporting Information

Microfluidic particle engineering of hydrophobic drug with Eudragit E100 - bridging the amorphous and crystalline gap

Swati Shikha [1], *Yi Wei Lee*[2,3], *Patrick S. Doyle*[1,4,5*], and *Saif A. Khan*[2*]

1 Critical Analytics for Manufacturing Personalized-Medicine, Singapore-MIT Alliance for Research and Technology, Singapore 138602, Singapore

2 Department of Chemical and Biomolecular Engineering, National University of Singapore, 4 Engineering Drive 4, Singapore 117576, Singapore

3 NUS Graduate School for Integrative Sciences & Engineering, National University of Singapore, Singapore 119077, Singapore

4 Department of Chemical Engineering, Massachusetts Institute of Technology, Cambridge, Massachusetts 02139, USA

5 Harvard Medical School Initiative for RNA Medicine, Boston, MA 02215, USA

*__Corresponding Authors__:

Email: Saif A. Khan (saifkhan@nus.edu.sg) and Patrick Doyle (pdoyle@mit.edu)

Supplementary Video S1. Powder flow of raw NPX, neat NPX microparticles, and co-processed E100-NPX 0.25 microparticles in glass vials.

1. Residual solvent analysis in E100-NPX microparticles

The amount of residual solvent (moisture and DCM) is critical for the long-term stability of the API in the formulation. Additionally, DCM could have potential toxicity risks as it belongs to FDA's class 2 of solvent classification.[1]

Residual moisture content was analysed using TGA and a plot of change in mass fraction against temperature change was obtained (**Figure S1a**). Based on the mass loss observed until 100 °C, the residual moisture content in E100-NPX 0.25 microparticles was found to be 2.5% (w/w). Residual DCM was quantified for dried E100-NPX 0.25 microparticles using benchtop proton NMR and the data was analyzed using Spectrus Processor 2021.1.2 from ACD/Labs. Typically, the proton NMR peak for pure DCM emerges around 5.3 ppm (**Figure S1b**). Spectra for E100-NPX 0.25 microparticles, however, did not show any DCM peak (**Figure S1c**) and the amount of residual DCM was found to be lower than the limit of detection of the equipment which is 50 µM or ~3.2 µg. For ~10 mg of E100-NPX 0.25 microparticles used, 80% NPX content amounts to 8 mg of the total drug, relative to which residual DCM is 0.04% w/w. Considering NPX dosage as 1000 mg/day (typical) to 1500 mg/day (maximum)[2], residual DCM amount in E100-NPX 0.25 microparticles was found to be 0.4- 0.6 mg/day.

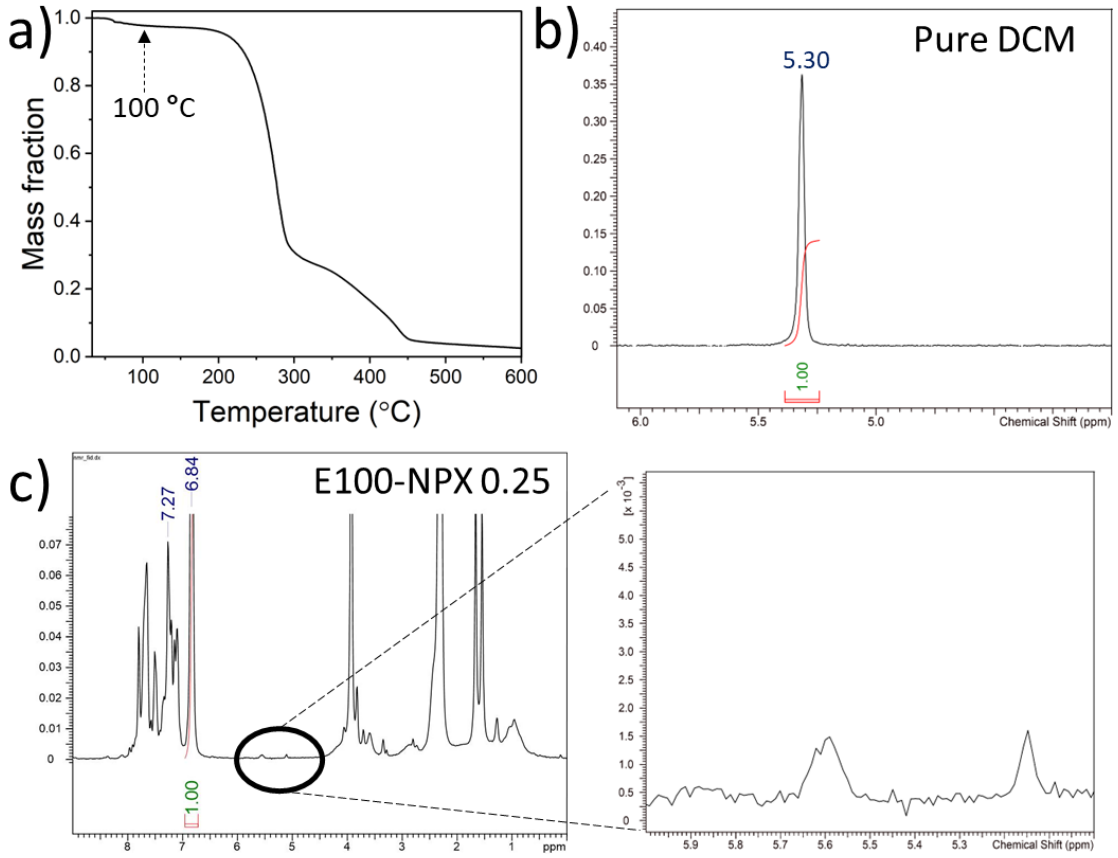

Figure S1. Residual solvent characterization (a) TGA curve of E100-NPX 0.25 microparticles showing residual moisture, and proton NMR spectra of (b) pure DCM and (c) E100-NPX 0.25 microparticles with the zoomed-in inset showing an absence of peak for DCM at 5.3 ppm.

2. Gordon-Taylor equation

The Gordon-Taylor equation (1) is used to predict the glass transition temperature of amorphous drug-polymer mixtures to understand the composition-dependent miscibility:[3]

$$T_g = \frac{w_1 T_{g_1} + k w_2 T_{g_2}}{w_1 + k w_2}, \; k = \frac{\rho_1 T_{g_1}}{\rho_2 T_{g_2}} \qquad (1)$$

where, ρ_1, T_{g_1}, w_1 *and* ρ_2, T_{g2}, w_2 are density, glass transition temperature, and weight fraction of Eudragit E100 and amorphous NPX, respectively. Density of E100 was taken as 1.09 g/cm^3, as reported earlier.[4, 5] Density and glass transition temperature of NPX was taken as 1.27 g/cm^3 and 6 °C, respectively, as reported earlier.[6, 7] T_g values calculated from the Gordon-Taylor equation for E100-NPX microparticles were found to be higher than those

obtained experimentally from the second heat cycle of DSC as presented in **Figure S2**. This positive deviation from the ideal mixing of the components suggested that the interactions between drug-polymer are greater compared to the interaction between the individual components that were inferred to be ionic in nature based on the ATR-FTIR findings.[3]

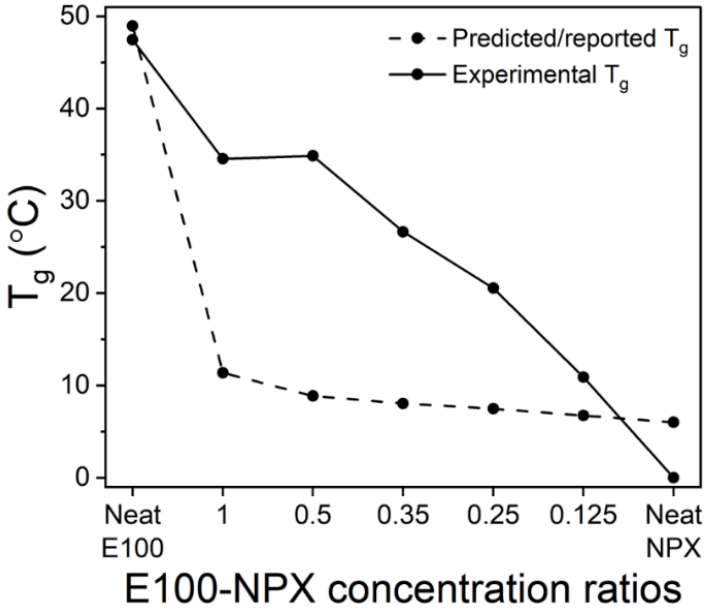

Figure S2. Experimental (based on second heat scan of DSC) and predicted (using Gordon-Taylor equation) glass transition temperatures (T_{gs}) plotted against different concentration ratios of E100-NPX microparticles.

3. Size distribution (bright-field microscopy images) and spatial drug distribution (Raman mapping)

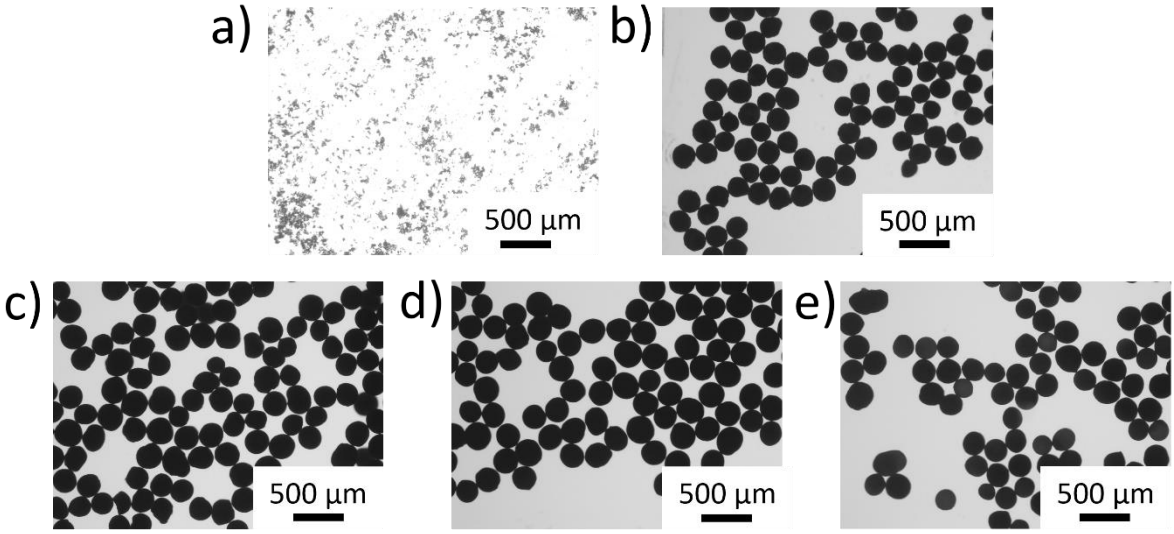

Figure S3. Bright-field microscopy images of (a) raw NPX, (b) neat NPX, (c) E100-NPX 0.125, (d) E100-NPX 0.25, and (e) E100-NPX 0.35 microparticles.

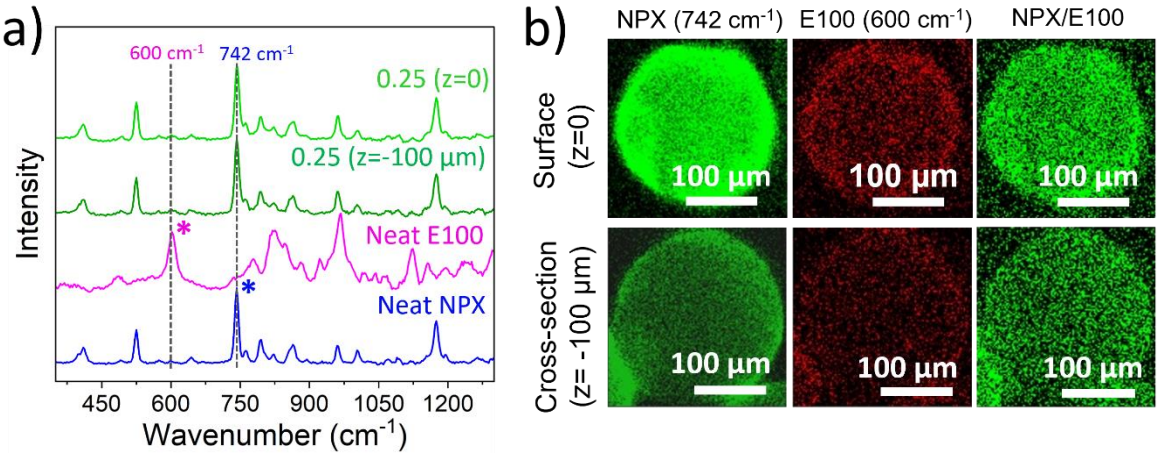

Figure S4. Spatial drug distribution in E100-NPX 0.25 microparticles (a) Raman spectra with specific peaks for E100 at 600 cm^{-1} (pink asterisk) and for NPX at 742 cm^{-1} (blue asterisk) in neat E100, neat NPX, and surface and at a confocal depth of ~100 µm for E100-NPX 0.25 microparticles (b) Confocal Raman maps for the peak intensity ratio of 742 cm^{-1} (NPX)/600 cm^{-1} (E100) showing uniform drug distribution on the surface and optical cross-section of E100-NPX 0.25 microparticles.

4. Primary particles size distribution and porosity of neat NPX and E100-NPX 0.25 microparticles

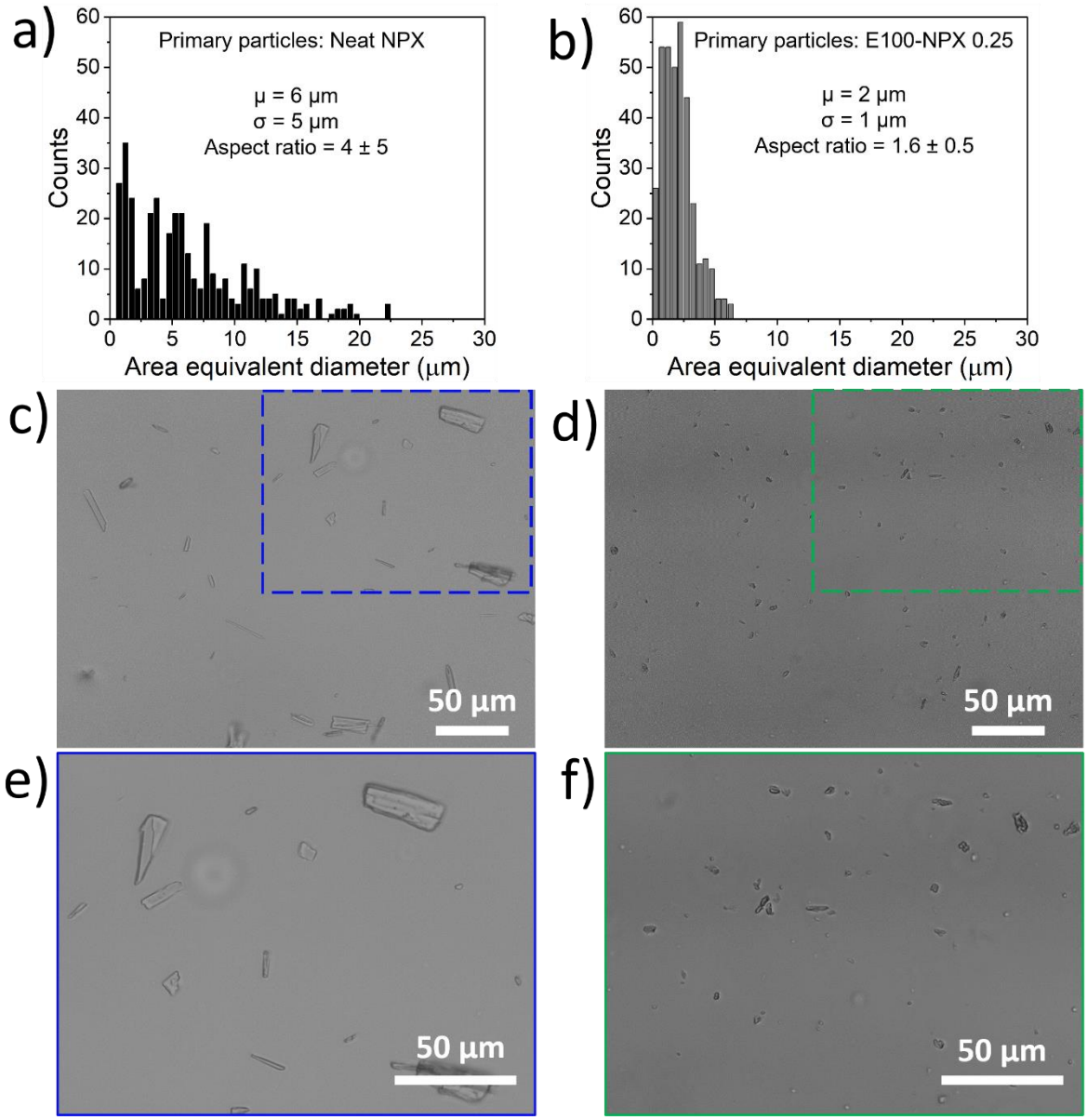

Figure S5. Size and size distribution of primary particles for (a) neat NPX and (b) E100-NPX 0.25 microparticles, and bright field images of primary particles in solution for (c) neat NPX, and (d) E100-NPX 0.25 microparticles. Images (e) and (f) are zoomed-in versions of selected areas from images (c) and (d), respectively.

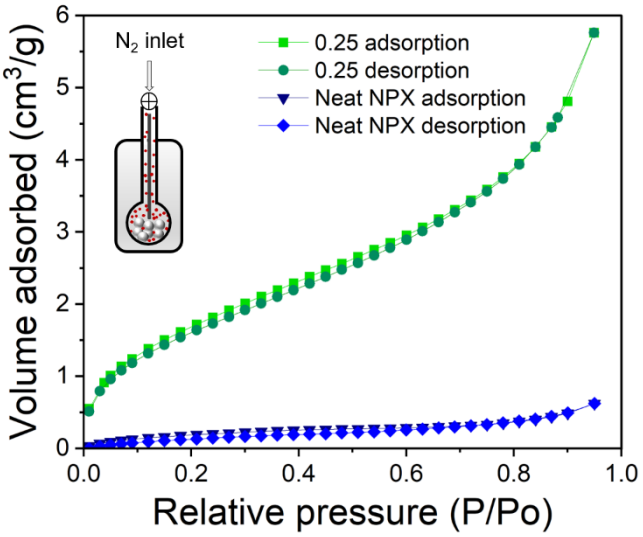

Figure S6. Nitrogen (N_2) adsorption and desorption isotherms for neat NPX (blue curves) and E100-NPX 0.25 (green curves) microparticles. The inset schematic illustrates the BET setup.

5. Drug loading and drug release

Table S1. Drug loading and entrapment efficiency for co-processed E100-NPX microparticles. Data presented are averaged across triplicates for each group.

E100-NPX crystalline formulations	Theoretical drug loading	Experimental drug loading	Entrapment efficiency
E100-NPX 0.125	89%	89.9 ± 1.5%	101 ± 1.7 %
E100-NPX 0.25	80%	81.1 ± 2 %	101.3 ± 2.5 %
E100-NPX 0.35	74%	73.5 ± 0.9 %	99.3 ± 1.3 %

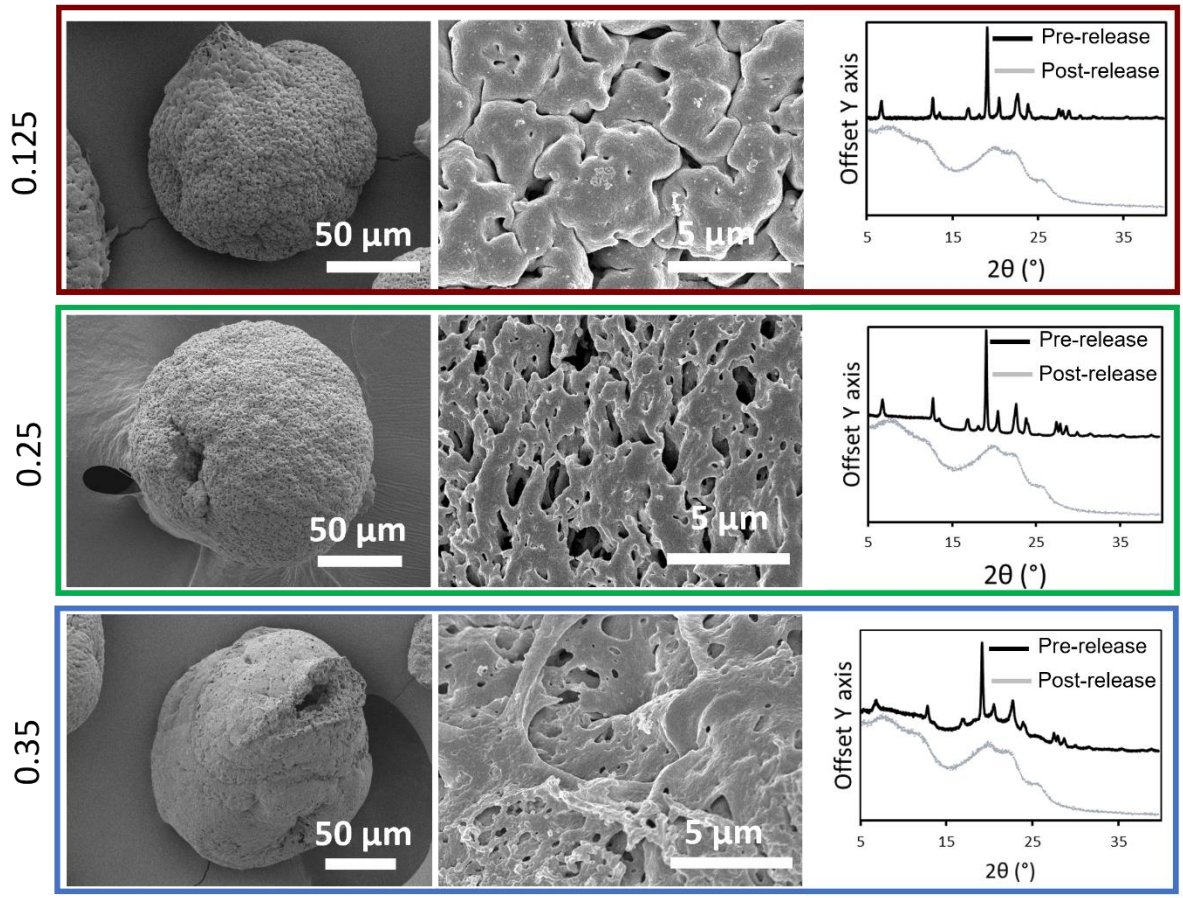

Figure S7. Surface FESEM images and PXRD spectra of E100-NPX 0.125 (top panel), 0.25 (middle panel), and 0.35 (bottom panel) remnant microparticles recovered after release in pH 7.4.

For further clarity, the release profiles of E100-NPX microparticles were compared with neat NPX using FDA recommended difference ($f1$) and similarity ($f2$) factors for release data at both the pH values using the equations (2) and (3) below[8-11].

$$f1 = \{[\sum_{t=1}^{n}|R_t - T_t|]/[\sum_{t=1}^{n} R_t]\} \times 100 \quad (2)$$

$$f2 = 50\ \log_{10}\left\{\left[1 + \left(\frac{1}{n}\right)\sum_{t=1}^{n}(R_t - T_t)^2\right]^{-0.5} \times 100\right\} \quad (3)$$

where, R_t and T_t represent percent drug release from neat NPX and E100-NPX microparticles, respectively at time t, and n is the total number of release time points. While $f1$ measures the percentage difference between the two release profiles, $f2$ measures the similarity and is a logarithmic reciprocal square root transformation of the sum of squared errors of differences.

For similarity, the two release profiles being compared should have 0< $f1$<15 and 50< $f2$<100.[8-10] The values of $f1$ and $f2$ are summarized in **Table S2**. For pH 7.4, similar release was observed from E100-NPX 0.125 ($f1$, 3; $f2$, 72) and 0.25 ($f1$, 7; $f2$, 63) microparticles compared to that of neat NPX. However, a significantly higher $f1$ (27) and lower $f2$ (34) values for E100-NPX 0.35 indicated differences in release profiles which was attributed to the delayed release from these microparticles owing to the higher concentration of polymer which is insoluble at this pH. On the other hand, for pH 1.2, the higher $f1$ and lower $f2$ values for all the co-processed E100-NPX microparticles indicated difference in release profiles compared to the neat NPX microparticles. The total number of release time points for calculating the difference/similarity factors was 3 for pH 7.4 (5, 10, and 15 minutes) and 8 for pH 1.2 (from 15 minutes to 4 hours).

Table S2. Drug release kinetics, and difference ($f1$) and similarity ($f2$) factors for neat NPX in comparison to E100-NPX 0.125, 0.25, and 0.35 microparticles in release media with pH 7.4 (PBS, neutral) and pH 1.2 (SGF, acidic).

Formulations	pH 7.4 (PBS)			pH 1.2 (SGF)		
	Release rate constant ($x10^{-3}$) (min^{-1})	f1 factor	f2 factor	Release rate constant ($x10^{-3}$) (min^{-1})	f1 factor	f2 factor
Neat NPX	0.19	-	-	3.8	-	-
E100-NPX 0.125	0.17	3	72	6	33	47
E100-NPX 0.25	0.14	7	63	6	29	50
E100-NPX 0.35	0.08	27	34	6	36	46

To understand the release behavior at non-sink conditions, microparticles with and without excipients (neat NPX and E100-NPX 0.25) were weighed such that the final concentration of NPX for both the samples was ~20 µg/mL in 80 mL of SGF (pH 1.2). The study was conducted on an orbital shaker (PSU-10i, Biosan) at 200 rpm at room temperature. For both the samples, 1 mL of release media was carefully pipetted out at predetermined time intervals to measure

the apparent free drug release using Cary 60 UV–visible spectrophotometer, and 1 mL of fresh media was added to maintain the constant release volume. In contrast to the release at sink conditions, both E100-NPX 0.25 and neat NPX microparticles were intact even after 24 hours. However, release from E100-NPX 0.25 microparticles was still faster than that of neat NPX. This highlights the potential impact of E100 in enhancing the release from the co-processed microparticles at lower release volume at pH 1.2.

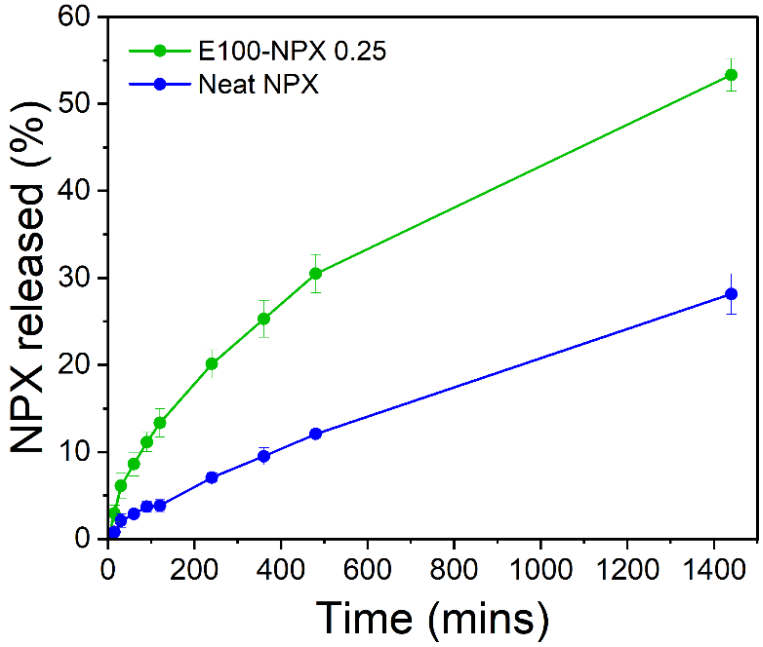

Figure S8. Release profiles of neat NPX and E100-NPX 0.25 at pH 1.2, room temperature, under non-sink conditions (error bars correspond to standard deviations for triplicates for each group).

References

1. *International Council For Harmonisation Of Technical Requirements For Pharmaceuticals for Human Use.* IMPURITIES: GUIDELINE FOR RESIDUAL SOLVENTS Q3C(R8), 2021. https://database.ich.org/sites/default/files/ICH_Q3C-R8_Guideline_Step4_2021_0422_1.pdf (accessed 23 May 2022).

2. Abraham, N. S.; El–Serag, H. B.; Johnson, M. L.; Hartman, C.; Richardson, P.; Ray, W. A.; Smalley, W. National adherence to evidence-based guidelines for the prescription of nonsteroidal anti-inflammatory drugs. *Gastroenterology* **2005**, *129* (4), 1171-1178.

3. Gordon, M.; Taylor, J. S. Ideal copolymers and the second-order transitions of synthetic rubbers. I. Non-crystalline copolymers. *Journal of Applied Chemistry* **1952**, *2* (9), 493-500.

4. Six, K.; Leuner, C.; Dressman, J.; Verreck, G.; Peeters, J.; Blaton, N.; Augustijns, P.; Kinget, R.; Van den Mooter, G. Thermal properties of hot-stage extrudates of itraconazole and eudragit E100. Phase separation and polymorphism. *Journal of Thermal Analysis and calorimetry* **2002**, *68* (2), 591-601.

5. Janssens, S.; De Zeure, A.; Paudel, A.; Van Humbeeck, J.; Rombaut, P.; Van den Mooter, G. Influence of preparation methods on solid state supersaturation of amorphous solid dispersions: a case study with itraconazole and eudragit e100. *Pharmaceutical research* **2010**, *27* (5), 775-785.

6. Paudel, A.; Van den Mooter, G. Influence of solvent composition on the miscibility and physical stability of naproxen/PVP K 25 solid dispersions prepared by cosolvent spray-drying. *Pharmaceutical research* **2012**, *29* (1), 251-270.

7. Allesø, M.; Chieng, N.; Rehder, S.; Rantanen, J.; Rades, T.; Aaltonen, J. Enhanced dissolution rate and synchronized release of drugs in binary systems through formulation: Amorphous naproxen–cimetidine mixtures prepared by mechanical activation. *Journal of Controlled Release* **2009**, *136* (1), 45-53.

8. Lam, M.; Ghafourian, T.; Nokhodchi, A. Optimising the release rate of naproxen liqui-pellet: a new technology for emerging novel oral dosage form. *Drug Delivery and Translational Research* **2020**, *10* (1), 43-58.

9. Rocha, H. V. A.; de Sousa Augusto, R.; Prado, L. D.; de Carvalho, E. M. Characterization of nimesulide and development of immediate release tablets. *Eclética Química* **2019**, *44* (3), 20-35.

10. Jammula, S.; Patra, C. N.; Swain, S.; Panigrahi, K. C.; Nayak, S.; Dinda, S. C.; Rao, M. E. B. Design and characterization of cefuroxime axetil biphasic floating minitablets. *Drug Delivery* **2015**, *22* (1), 125-135.

11. Moore, J.; Flanner, H. Mathematical comparison of dissolution profiles. *Pharmaceutical technology* **1996**, *20* (6), 64-74.